HHS Public Access

Author manuscript

Nat Med. Author manuscript; available in PMC 2015 November 01.

Published in final edited form as:

Nat Med. 2015 May ; 21(5): 457–466. doi:10.1038/nm.3839.

Active Pin1 is a key target of all-*trans* retinoic acid in acute promyelocytic leukemia and breast cancer

Shuo Wei[1,2], **Shingo Kozono**[1,2], **Lev Kats**[1,2,3], **Morris Nechama**[1,2], **Wenzong Li**[4], **Jlenia Guarnerio**[1,2,3], **Manli Luo**[1,2], **Mi-Hyeon You**[5], **Yandan Yao**[1,2], **Asami Kondo**[1,2], **Hai Hu**[1,2], **Gunes Bozkurt**[6], **Nathan J. Moerke**[7], **Shugeng Cao**[5], **Markus Reschke**[1,2,3], **Chun-Hau Chen**[1,2], **Eduardo M. Rego**[9], **Francesco LoCoco**[10], **Lewis Cantley**[2], **Tae Ho Lee**[5], **Hao Wu**[6], **Yan Zhang**[4], **Pier Paolo Pandolfi**[1,2,3], **Xiao Zhen Zhou**[1,2,11], and **Kun Ping Lu**[1,2,11]

[1]Cancer Research Institute, Beth Israel Deaconess Cancer Center, Beth Israel Deaconess Medical Center, Harvard Medical School, Boston, MA, USA

[2]Department of Medicine, Beth Israel Deaconess Medical Center, Harvard Medical School, Boston, MA, USA

[3]Department of Pathology, Beth Israel Deaconess Medical Center, Harvard Medical School, Boston, MA, USA

[4]Department of Molecular Biosciences, University of Texas, Austin, TX, USA

[5]Division of Gerontology, Department of Medicine, Beth Israel Deaconess Medical Center, Boston, Massachusetts, USA

[6]Department of Biological Chemistry and Molecular Pharmacology, Harvard Medical School, Boston, MA, USA

[7]Department of Systems Biology, Harvard Medical School, Boston, MA, USA

[8]Department of Biological Chemistry and Molecular Pharmacology, Harvard Medical School, Boston, MA, USA

[9]Department of Internal Medicine, University of São Paulo, Ribeirão Preto, Brazil

[11]Correspondence to: Kun Ping Lu, klu@bidmc.harvard.edu or Xiao Zhen Zhou, xzhou@bidmc.harvard.edu.

CONTRIBUTIONS

S.W. designed the studies, performed the experiments, interpreted the data, and wrote the manuscript; S.K. helped characterize ATRA binding to and inhibiting Pin1; L.K., J.G. and M.R. helped design and conduct APL-related experiments; W.L. and Y.Z. determined the Pin1-ATRA co-crystal structure; M.N., M. L., Y.Y., A. K., H.H., and C.H.C. provided various technical assistances; M.H.Y and T.H.L. performed Pin1 and DAPK1 immunostaining; G.B. and H.W. helped analyze Pin1 and ATRA binding; N.J.M. and S.C. provided advice on FP-HTS screen; E.M.R. and F.L. provided human APL samples; L.C.C. advised the project; P.P.P. advised the project, interpreted the data and reviewed the manuscript; X.Z.Z. developed the original Pin1 FP-HTS and worked with S.W. to identify ATRA; X.Z.Z. and K.P.L. conceived and supervised the project, designed the studies, interpreted the data, and wrote the manuscript.

LIST OF THE SUPPLEMENTARY MATERIALS

11 Supplemental Figures

4 Supplemental Tables

Online Methods

[10]Department of Biomedicine and Prevention, Tor Vergata University and Santa Lucia Foundation, Rome, Italy

Abstract

A common key regulator of oncogenic signaling pathways in multiple tumor types is the unique isomerase Pin1. However, available Pin1 inhibitors lack the required specificity and potency. Using mechanism-based screening, here we find that all-*trans* retinoic acid (ATRA)--a therapy for acute promyelocytic leukemia (APL) that is considered the first example of targeted therapy in cancer, but its drug target remains elusive--inhibits and degrades active Pin1 selectively in cancer cells by directly binding to the substrate phosphate- and proline-binding pockets in the Pin1 active site. ATRA-induced Pin1 ablation degrades the fusion oncogene PML-RARα and treats APL in cell and animal models and human patients. ATRA-induced Pin1 ablation also inhibits triple negative breast cancer cell growth in human cells and in animal models by acting on many Pin1 substrate oncogenes and tumor suppressors. Thus, ATRA simultaneously blocks multiple Pin1-regulated cancer-driving pathways, an attractive property for treating aggressive and drug-resistant tumors.

Targeted therapy has changed cancer treatment, but blocking a single pathway is often ineffective against solid tumors, especially aggressive or drug-resistant ones due to activation of redundant and/or alternative oncogenic pathways[1]. Thus a major challenge remains how to block the multiple cancer-driving pathways simultaneously. A common and central signaling mechanism in oncogenic pathways is proline-directed phosphorylation (pSer/Thr-Pro)[2]. Numerous oncogenes and tumor suppressors are either directly regulated by such phosphorylation (Supplementary Fig. 1) and/or trigger signal pathways involving such phosphorylation[2,3]. Notably, the same kinases often phosphorylate both oncogenes and tumor suppressors to control their function. The prolyl isomerase (PPIase) Pin1 plays a critical role in coordinating these multiple phosphorylation events to oncogenesis[2,3].

Proline uniquely adopts *cis* and *trans* conformations, and their isomerization is catalyzed by PPIases[4] including the unique PPIase Pin1[2,5,6]. Using its WW domain, Pin1 binds to specific pSer/Thr-Pro motif(s), where its PPIase domain catalyzes *cis-trans* isomerization of certain pSer/Thr-Pro motifs[5], which can be detected by *cis* and *trans*-specific antibodies[6]. Pin1 is commonly overexpressed and/or activated in human cancers, which correlates with poor outcomes[3,7]. In contrast, the Pin1 polymorphisms that lower Pin1 are associated with reduced cancer risk[8]. Moreover, Pin1 deficiency in mice prevents tumorigenesis, even that induced by activated oncogenes such as HER2 or Ras[9], whereas Pin1 overexpression disrupts cell cycle coordination leading to centrosome amplification, chromosome instability and cancer development in cell and animal models of breast cancer[10]. Pin1 activates at least 32 oncogenes and growth-promoting proteins, and inactivates at least 19 tumor suppressors and growth-inhibiting proteins[2,3,11–20] (Supplementary Fig. 1). Thus, Pin1 can amplify oncogenic pathways by simultaneously activating oncogenes and inactivating tumor suppressors. Pin1 also plays a fundamental role in driving expansion and tumorigenesis of cancer stem cells[21–23], a major source of cancer resistance[1]. These results suggest that Pin1 inhibitors could have the unique and desirable ability to block multiple cancer-driving pathways as well as inhibit cancer stem cells at the same time[2,3,24], especially given that

Pin1 KO mice develop normally without obvious defects for an extended period of time[25,26].

However, the available Pin1 inhibitors lack the required specificity and/or potency, or cannot efficiently enter cells[3,27]. Here we develop mechanism-based high throughput screening for compounds targeting active Pin1. We find that ATRA (all-*trans* retinoic acid, tretinoin) directly binds, inhibits and ultimately degrades active Pin1, thereby exerting potent anticancer activity against APL and triple negative breast cancer (TNBC) by simultaneously blocking multiple Pin1-regulated cancer-driving pathways.

RESULTS

Mechanism-based screening for Pin1 inhibitors

Phosphorylation of Pin1 on S71 by the tumor suppressor DAPK1[28] inhibits Pin1 catalytic activity and oncogenic function by blocking a phosphorylated substrate from entering the active site[7] (Supplementary Fig. 2a). Such phosphorylation would likely also prevent Pin1 from binding to pTide, a high affinity substrate-mimicking peptide inhibitor (Bth-D-phos.Thr-Pip-Nal with Kd of 1.2 nM) that cannot enter cells[7,29] (Supplementary Fig. 2b). Indeed, fluorescently-labeled pTide bound to Pin1, but not to FKBP12 (FK506-binding protein 12), and to the Pin1 PPIase domain, but not to its WW domain (Supplementary Fig. 2c–f). pTide also bound to the nonphosphorylatable Pin1 S71A mutant, but not to its phospho-mimicking S71E mutant; binding depending on Pin1 active site residues including K63 and R69 that mediate phosphate binding, and L122, M130, Q131 and F134 that mediate Pro recognition[29] (Supplementary Fig. 2g). Thus, we developed a fluorescence polarization-based high-throughput screen (FP-HTS) to screen for chemical compounds that could compete with pTide for binding to the non-phosphorylated (and thus active) Pin1. Out of ~8200 compounds screened, 13-*cis*-retinoic acid (13cRA) was the top hit based on lowest Z score (Fig. 1a).

13cRA and its isomer, ATRA (Fig. 1b, c), bound to Pin1 in the FP assay, with ATRA being more potent after a short period of incubation with Pin1, with calculated Ki values being 1.16 and 0.58 μM (Supplementary Fig. 3a) using an equation as described[30], but this difference disappeared after a longer incubation (Supplementary Fig. 3b, c). These results suggest that Pin1 may mainly bind to the *trans* form (ATRA) and can bind to the *cis* form (13cRA) after it is converted to *trans*, which does occur over time *in vitro* and *in vivo*[31]. The ATRA-Pin1 interaction was confirmed using a different fluorescence labeled pTide probe (Supplementary Fig. 2h). Since [^{3}H]-ATRA has been used as a photoaffinity labeling reagent to covalently and specifically tag ATRA-binding proteins[32], we performed photoaffinity labeling of Pin1 with [^{3}H]ATRA, followed by detecting the binding using SDS-containing gels. [^{3}H]-ATRA directly bound to Pin1, with Kd = 0.80 μM (Fig. 1d, e and Supplementary Fig. 3a), confirming their direct binding. Moreover, ATRA and 13cRA fully inhibited PPIase activity of Pin1, with Ki values being 0.82 and 2.37 μM, respectively (Fig. 1f and Supplementary Fig. 3a, d, e), similar to those in the FP assay, but neither inhibited other major PPIases cyclophilin and FKBP12 (Supplementary Fig. 3f, g). Thus ATRA is a submicromolar Pin1 inhibitor.

ATRA binds to the Pin1 active site

To determine whether the carboxylic acid in ATRA serves as an alternative to the phosphate group for binding to Pin1, several structurally similar retinoids with substituted carboxylic or aromatic groups, and the new generations of retinoids fenretinide[33] and bexarotene[34], were tested for Pin1 binding. ATRA was the most potent against Pin1 out of those tested (Fig. 1g and Supplementary Fig. 4a). Notably, carboxylic acid group (-COOH)-substituted retinoids, including retinol (-OH), retinyl acetate (-$OCOCH_3$) and retinal (-CHO) were totally inactive (Fig. 1g and Supplementary Fig. 4a). In line with this idea, fenretinide and bexarotene showed only marginal Pin1 binding (Fig. 1g and Supplementary Fig. 4a), which might be due to the lack of carboxyl and/or modifications to target RARs, RXRs or others[33–35].

To understand how ATRA inhibits Pin1 catalytic activity, we determined the co-crystal structure of ATRA and the Pin1 PPIase domain (Supplementary Fig. 4b and Supplementary Table 1). After ATRA soaking, strong electron density was observed at the Pin1 active site (Fig. 1h). The most well-defined region of ATRA was its carboxyl group, which formed salt bridges with the critical catalytic residues K63 and R69 (Fig. 1i *right*), both of which are essential for binding the phosphate group in the Pin1 substrate[29]. At the high resolution of 1.3 Å, two alternative conformations of R69 were visible, both of which were within the distance range of salt bridge formation with the carboxyl group of ATRA. The trimethyl cyclohexene ring of ATRA was sandwiched in the hydrophobic Pro-binding pocket formed by L122, M130, Q131 and F134 of Pin1[29] (Fig. 1i *left*). Notably, the binding modes of ATRA and pTide overlapped (Fig. 1i and Supplementary Fig. 2b). Thus, by mimicking the pSer/Thr-Pro motif in a substrate, the carboxylic and aromatic moieties of ATRA bind to the substrate phosphate- and proline-binding pockets of the Pin1 active site, respectively. These structural requirements are also consistent with our findings that the carboxyl group of ATRA is required for binding to Pin1 and that fenretinide and bexarotene are less potent than ATRA in binding Pin1 (Fig. 1g).

ATRA induces Pin1 degradation and inhibits its function

To determine whether ATRA inhibits Pin1 activity in cells, we first compared its effects on the proliferation of Pin1 KO ($Pin1^{-/-}$) and wild-type (WT, $Pin1^{+/+}$) MEFs. Relatively high concentrations of ATRA were required to inhibit the growth of Pin1 WT MEFs, and Pin1 KO cells were more resistant to ATRA (Fig. 2a *left*). Susceptibility to ATRA was fully restored by re-expressing Pin1, but not its inactive W34/K63A mutant (Fig. 2a *right*). Notably, ATRA also dose-dependently down-regulated WT but not mutant Pin1 (Fig. 2b). ATRA had no obvious effects on Pin1 mRNA levels (Fig. 2c). ATRA reduced both exogenous and endogenous Pin1, but not the W34/K63A mutant that did not bind ATRA (Fig. 2b and Supplementary Fig. 2g). ATRA-induced Pin1 degradation was suppressed by the proteasome inhibitor MG132 (Fig. 2d), and ATRA and 13cRA reduced Pin1 protein half-life (Fig. 2e) with ATRA being more potent (Fig. 2b, e).

Next we examined the effects of ATRA on the well-documented oncogenic phenotypes induced by Pin1 overexpression, such as centrosome amplification[10], activation of the cyclin D1 promoter[11] and enhanced foci formation; all of these phenotypes are inhibited by

DAPK1-mediated S71 phosphorylation of Pin1[7]. ATRA dose-dependently and fully inhibited the ability of Pin1 overexpression to induce centrosome amplification in NIH 3T3 cells (Fig. 2f, g), and its ability to activate the cyclin D1 promoter (Fig. 2h) and enhance foci formation (Fig. 2i, j) in SKBR3 cells. Thus, ATRA induces Pin1 degradation and inhibits its oncogenic function.

Pin1 is a key target of ATRA in APL cells

ATRA is approved to treat APL, where it activates retinoic acid receptors (RARs) to induce APL cell differentiation and also causes degradation of the fusion protein promyelocytic leukemia (PML)/retinoic acid receptor (PML-RARα) to inhibit self-renewal of APL stem cells[36–38]. However, the ATRA-induced RARα activation can be decoupled from its ability to induce PML-RARα degradation and to treat APL[39,40]. Notably, retinoid analogs that potently activate RARs and induce leukemia cell differentiation, but fail to induce PML-RARα degradation, also fail to inhibit leukemia stem cells and treat APL[40]. Moreover, ATRA's ability to activate RARs cannot readily explain its activity to stabilize other oncogenic molecules, including cyclin D1[41] and NFκB[42], and to destabilize tumor suppressive molecules such as Smad[43]. Thus, the target(s) of ATRA that mediate the anticancer effects remain elusive.

To examine the role of RARs in ATRA-directed degradation of PML-RARα, we used a pan-RAR agonist, AC-93253, and a pan-RAR inhibitor, Ro-415253, which are structurally distinct from ATRA (Supplementary Fig. 5a) and exhibit the expected ability to activate or inhibit transcription of RAR downstream targets, respectively (Supplementary Fig. 5b). Ro-415253 showed minimal Pin1 binding, and AC-93253 showed no binding (Supplementary Fig. 5c). The pan-RAR inhibitor did not prevent ATRA from inducing degradation of Pin1 or PML-RARα (Supplementary Fig. 5d) or inhibit the growth of human APL NB4 cells[44] (Supplementary Fig. 5e), while the pan-RAR activator did not mimic ATRA-induced Pin1 or PML-RARα degradation (Supplementary Fig. 5f). These RAR-independent ATRA effects were also confirmed using RARα, β, γ triple KO MEFs[40], in which ATRA induced degradation of PML-RARα and Pin1 similarly to in WT controls (Supplementary Fig. 5g, h).

ATRA-induced PML-RARα degradation is associated with phosphorylation on the Ser581-Pro motif of PML-RARα[39], which corresponds to the Pin1 binding site pSer77-Pro in RARα[45]. Since Pin1 binds to and increases protein stability of numerous oncogenes[2,3] (Supplementary Fig. 1), we hypothesized that Pin1 might bind to the pS581-Pro motif in PML-RARα and stabilize it, thereby promoting APL cell growth. Indeed, Pin1 interacted with PML-RARα and the S581A but not S578A mutation abolished this interaction (Supplementary Fig. 6a) and reduced PML-RARα stability (Supplementary Fig. 6b, c)[2,3]. Moreover, Pin1 knockdown using a shRNA-containing lentivirus[7] reduced PML-RARα stability and inhibited APL cell growth; both effects were rescued by re-expression of shRNA-resistant Pin1, but not its inactive mutant (Fig. 3a–e). In contrast to PML-RARα, Pin1 interacted much less with PLZF-RARα (Supplementary Fig. 7a), and Pin1 shRNA knockdown only marginally reduced protein stability of PLZF-RARα (Supplementary Fig. 7b–e). Although future experiments are needed to define the underlying mechanisms, these

results are consistent with the fact that APL induced by PLZF-RARα is usually resistant to ATRA[36–38].

To expand our investigation beyond PML-RARα, we compared genome-wide gene expression profiles of ATRA and DMSO-treated NB4 cells, and NB4 cells stably expressing control or Pin1 shRNA using microarrays covering coding and non-coding transcripts in the human whole genome. Clustering analysis revealed similarity between ATRA-treated and Pin1 shRNA cells. 528 genes were differentially expressed both in Pin1 KD cells and ATRA-treated cells, as compared with their respective controls. 304 genes were upregulated including many growth-suppressors (e.g. PDCD4 and SORL1) and 224 downregulated including many growth-stimulators (e.g. CCL2, SPP1, IL1B and IL8) both in Pin1 KD cells and ATRA-treated cells (Fig. 3f and Supplementary Table 2). Thus, both PML-RARα gene-specific and genome-wide analyses support the idea that ATRA inhibits Pin1 in APL cells.

We corroborated these *in vitro* results in animal studies using sublethally irradiated immunodeficient NOD-SCID-Gamma (NSG) mice transplanted with NB4 cells stably expressing an inducible Tet-on shPin1[46]. When doxycycline-containing food was given 5 days post-transplantation and throughout the remaining course of the experiment, Pin1 and PML-RARα expression decreased in the bone marrow (Fig. 3g). In contrast to mice given control food, which exhibited splenomegaly, mice fed doxycycline displayed normal spleen size (Fig. 3h and Supplementary Fig. 8a). Doxycycline-fed mice also contained fewer human CD45-expressing NB4 cells in the bone marrow (Supplementary Fig. 8b–d). Disease-free survival of doxycycline-fed mice was also significantly extended compared to mice fed control chow (Fig. 3i). Notably, in one doxycycline-fed mouse that died early, Pin1 and PML-RARα were expressed in amounts close to those in mice not fed with doxycycline (Fig. 3j), supporting the role of Pin1 and its effects on PML-RARα in survival in APL mice. Thus, like ATRA, inducible Pin1 KD alone is sufficient to cause PML-RARα degradation and treat APL in animal models.

ATRA and Pin1 inhibition suppress APL growth

We compared the effects of ATRA to the effects of three structurally distinct Pin1 inhibitors (PiB[47], EGCG[48] and Juglone[49]) on human APL NB4 cells *in vitro*; the latters are less potent and also have other targets/toxicities[27]. Like ATRA, these agents dose-dependently reduced PML-RARα in human APL cells, although they inhibited Pin1 without degrading it (Fig. 4a). However, in contrast to ATRA or the pan-RAR activator, neither Pin1 inhibitors nor Pin1 shRNA induced human APL cell differentiation (Fig. 4b). These results were further supported by the observation that ATRA but not Pin1 shRNA induced expression of RAR target genes (Supplementary Fig. 5i); the minimal effect of Pin1 shRNA could be attributed to the stabilization of RAR protein upon Pin1 shRNA, as shown previously[45].

To examine the effects of these Pin1 inhibitors on APL in vivo, sublethally irradiated B6 mice were injected with APL cells isolated from hCG-PML-RARα transgenic mice expressing PML-RARα under the control of the myeloid/promyelocytic specific cathepsin-G gene promoter[50] and 5 days later were treated with EGCG or Juglone, or with ATRA-releasing pellets (5 mg 21 days in one pellet implanted subcutaneously in the back of mice). After 20 days after the start of treatment, we analyzed differentiation of APL cells from

bone marrows by flow cytometry. ATRA, but neither EGCG nor Juglone, induced APL cell differentiation (Fig. 4c). Moreover, ATRA, but neither EGCG nor Juglone, reduced Pin1 levels in the bone marrow (Fig. 4d), although the reduction was not as profound as observed *in vitro* (Fig. 4a), likely due to the presence of normal cells in the bone marrow, which were usually more resistant to ATRA (Fig. 2a and Fig. 5a, b and Supplementary Fig. 10a). Nevertheless, all three Pin1 inhibitors effectively reduced PML-RARα in the bone marrow (Fig. 4d) and treated APL, with spleen weights nearly at basal levels (Fig. 4e and Supplementary Fig. 8e). Unlike ATRA-treated animals, EGCG or Juglone-treated mice were rather sick, likely due to the fact that EGCG and Juglone have other toxic effects[27]. These results are consistent with the previous findings that ATRA's ability to activate RARs and induce leukemia cell differentiation can be uncoupled from its ability to degrade PML-RARα and treat APL[39,40].

Next we determined whether ATRA treatment degrades Pin1 and PML-RARα in APL cells in human patients. We used double immunostaining with antibodies against Pin1 and PML to detect Pin1 and PML-RARα abundance and localization in cells from the bone marrow of healthy individuals or APL patients before or after patient treatment with ATRA for 3 or 10 days, or in APL patients in complete remission (Supplementary Table 3), as described[7,51]. In contrast to healthy controls, Pin1 and PML-RARα were markedly overexpressed and distributed throughout the entire nucleus in all patients examined prior to treatment (Fig. 4f–h). After ATRA treatment, PML-RARα levels were significantly reduced, with the signal detected mainly in PML nuclear bodies (Fig. 4f), which represents endogenous PML protein and reflects good ATRA response[51]. Importantly, ATRA treatment caused a time-dependent reduction of Pin1 and PML-RARα, to ~40% or <10% after 3 or 10 days of treatment, respectively (Fig. 4f–h). Notably, PML-RARα/PML staining colocalized with Pin1 in APL cells. PML-RARα/PML was still diffusely distributed throughout the entire nucleus in APL cells containing more Pin1 (Fig. 4f, **red arrows**), but was almost exclusively localized to PML bodies (likely reflecting endogenous PML) in APL cells that contained less Pin1 (Fig. 4f, **yellow arrows**). Similar results were also obtained by treating human APL NB4 cells with ATRA *in vitro* (Supplementary Fig. 9). Notably, neither Pin1 nor PML-RARα was overexpressed in APL patients in complete remission (Fig. 4f–h). Thus, Pin1 inhibition by ATRA, other chemical compounds or shRNA caused PML-RARα degradation in APL mouse models and human APL cells *in vitro* and in human patients.

ATRA as a candidate breast cancer therapy

Given that Pin1 regulates numerous cancer-driving molecules in solid tumors (Supplementary Fig. 1), we hypothesized that ATRA might have anticancer activity against other malignancies. We explored this in breast cancer due to the substantial oncogenic role of Pin1 in this disease[9,10,12]. We first treated nine different human normal and breast cancer cell lines with ATRA, and examined cell proliferation by the colorimetric MTT assay. Non-transformed MCF10A and HMLE cells were highly resistant to ATRA, and different malignant cells showed differential susceptibility to ATRA (Fig. 5a).

Compared with normal MCF10 and HMLE cells, Pin1 was overexpressed in all breast cancer cells (Fig. 5b)[11]. These cells expressed similar levels of cytochrome P450-dependent

retinoic acid-4-hydroxylase (Fig. 5b) and its inhibitor liarazole resulted in generally additive effects with ATRA (Supplementary Fig. 10c), suggesting that differences in ATRA metabolism do not likely account for the observed difference in ATRA sensitivity. Since the Pin1-ATRA co-crystal structure revealed that the carboxyl group of ATRA formed salt bridges with K63 and R69 of Pin1 (Fig. 1i), both of which are responsible for binding the phosphate of pS71 Pin1[7] (Supplementary Fig. 2a and 10a), we examined the possibility that S71 phosphorylation affects ATRA sensitivity. Indeed, the levels of S71 phosphorylation in different cell lines inversely correlated with ATRA sensitivity (Fig. 5b). Given that S71 in Pin1 is phosphorylated by DAPK1[7], a tumor suppressor often lost in solid tumors[28], we examined expression of Pin1 and DAPK1 in human TNBC tissues (Supplementary Table 4). High Pin1 but low DAPK1 were detected in most breast cancer tissues with an inverse correlation (n=48) (Fig. 5c and Supplementary Fig. 10b).

To examine whether the inhibitory effects of ATRA on breast cancer cell growth are related to RAR activation, we again used Ro-415253 and AC-93253. As in APL cells, neither had obvious effects on the ability of ATRA to induce Pin1 degradation or inhibit proliferation of breast cancer cells (Supplementary Fig. 10d–g).

To further support the thesis that ATRA targets Pin1 in breast cancer, we next examined the effect of ATRA on abundance of a set of oncogenes and tumor suppressors whose protein stability is regulated by Pin1 in breast cancer[2,3]. Indeed, ATRA caused a dose-dependent decrease in abundance of Pin1 and its substrate oncogenes including cyclin D1[12], HER2[14], ERα[18] Akt[16], NFκB p65[13], c-Jun[11], and PKM2[19], as well as an increase in abundance of Pin1 substrate tumor suppressors such as Smad2/3[17] and SMRT[15] in all three ATRA-sensitive cancer cell lines (Fig. 5d). ATRA had no appreciable effects on MCF10A cells (Fig. 5d). To further support the notion that these effects are due to Pin1 ablation, we stably introduced tetracycline-inducible Pin1 shRNA into these cells. Inducible Pin1 knockdown produced similar effects on the oncogenes and tumor suppressors as ATRA (Fig. 5d, e); these effects were rescued by reconstitution of shRNA-resistant Pin1, but not its W34/K63A mutant (Fig. 5f). Thus, ATRA selectively ablates active non-phosphorylated Pin1 and thereby inhibits multiple cancer-driving pathways in ER-positive, HER2-positive and triple negative human breast cancer cells.

To determine if ATRA inhibits breast tumor growth *in vivo*, we used MDA-MB-231 and MDA-MB-468 human TNBC cell lines; we selected TNBC because it has the worst prognosis and fewest treatment options. In pilot experiments, MDA-MB-231 cells were subcutaneously injected into the flank of female nude mice, and a week later mice were treated with 33.0 μmol/kg, or vehicle intraperitoneally 3 times a week for 8 weeks. ATRA had only modest antitumor activity (Supplementary Fig. 10h), which is consistent with the findings that ATRA had moderate efficacy against advanced breast cancer in clinical trials[35,52]; this could be due to its short half-life of ~45 min in humans[53].

We thus implanted ATRA-releasing or placebo pellets (to maintain a constant level of the drug) one week after TNBC cell lines were injected into the flank of nude mice. We followed tumor growth over eight weeks after implantation of ATRA pellets. ATRA potently and dose-dependently inhibited tumor growth and reduced abundance of Pin1 and

its substrate cyclin D1 in tumors derived from MDA-MB-231 cells (Fig. 6a, b) or MDA-MB-468 cells (Fig. 6c, d). Similar dose-dependent inhibition of tumor growth was observed when ATRA was first administered 3 weeks after MDA-MB-231 tumor cell inoculation, when tumors were already formed (Fig. 6e). To test whether the antitumor activity of ATRA against breast cancer is mediated by Pin1, we stably expressed Pin1 in MDA-MB-231 cells before injecting them into the flank of nude mice. Pin1 overexpression markedly increased tumor growth (by ~8 fold), which again was effectively inhibited by ATRA in a dose-dependent manner (Fig. 6f). ATRA also dose-dependently reduced both endogenous and exogenous Pin1 and endogenous cyclin D1 (Fig. 6g). Thus, ATRA has potent anti-tumor activity against TNBC through ablation of Pin1.

DISCUSSION

The use of ATRA in APL therapy has been described as the first example of targeted therapy in human cancer[36–38], but its drug target(s) remain elusive. Notably, retinoic acid-mediated transactivation is dispensable for leukemia initiated by PML-RARα[54]. ATRA's ability to activate RARs and induce leukemia cell differentiation can be uncoupled from its activity to induce PML-RARα degradation, inhibits APL stem cells and treat APL[39,40]. ATRA's ability to activate RARs cannot explain its activity to stabilize other oncogenic[41,42] and tumor suppressive[43] molecules. Finally, although regular ATRA with a half life of 45 min has moderate but detectable efficacy against solid tumors in some clinical trials, new generations of supposedly much more potent retinoid derivatives to target RARs or RXRs show little efficacy[35,52,55–57].

Our mechanism-based screening has led to the unexpected discovery that ATRA directly binds, inhibits and ultimately degrades active Pin1 selectively. This selectivity was confirmed by solving the Pin1-ATRA co-crystal structures, which reveal that the carboxylic and aromatic moieties of ATRA occupy the Pin1 substrate phosphate- and Pro-binding pockets in the Pin1 active site, respectively, and that S71 phosphorylation prevents ATRA from binding Pin1 by blocking the carboxyl-binding pocket. Notably, the ATRA carboxylic moiety mimics S71 phosphorylation by the tumor suppressor DAPK1, which inhibits Pin1 activity and oncogenic function[7]. Significantly, ATRA bound and inhibited Pin1 with Ki/Kd values of 0.5–0.8 μM *in vitro*. ATRA-releasing formulation effectively treated *in situ* APL and TNBC mouse models, which reportedly produces 0.6 μM drug concentration[40]. ATRA effectively degraded Pin1 and PML-RARα in APL cells in human patients at standard doses, which reportedly produce 1.2 μM[58]. Thus, Pin1 is a direct target for ATRA to induce PML-RARα degradation and to treat APL, likely being the long-sought-after target for ATRA in APL (Supplementary Fig. 11a). Of note, Gianni et al. reported that Pin1 inhibition enhances the responses of APL cells to ATRA via stabilization of PML-RARα[59], which is consistent neither with the previous findings that PML-RARα causes APL and that ATRA induces PML-RARα degradation to treat APL[39,40], nor our current findings that ATRA induces PML-RARα degradation by directly binding to and degrading Pin1. Moreover, Gianni et al[59] did not suggest that ATRA directly targets Pin1.

Our findings offer a promising new approach to targeting a common oncogenic mechanism to stop numerous cancer-driving molecules and inhibit cancer stem cells at the same time

(Supplementary Fig. 11a, b), which is critically needed for treating aggressive or drug-resistant cancers[1]. Although ATRA has only modest antitumor activity, ATRA-releasing pellets potently inhibit TNBC growth by ablating Pin1 and its targets. Notably, liposomal ATRA with a longer half-life has significant efficacy in APL patients even as a single-agent front-line therapy[60]. Consistent with the findings are that regular unmodified ATRA has moderate but detectable efficacy against advanced breast cancer in trials[35,52]. It would be interesting to examine whether cells from those patients who do respond show Pin1 degradation, and whether it could improve outcomes if one could select those patients. These results underscore the importance of developing longer half-life ATRA to improve its anticancer potency.

Our ATRA-Pin1 co-crystal structures provide insight into how ATRA binds to Pin1 by taking advantage of the substrate phosphate- and proline-binding pockets in the Pin1 active site. However, unlike a substrate, the carboxylic and aromatic moieties in ATRA are linked by double bonds, which cannot be isomerized by Pin1. As a result, ATRA may be trapped in the Pin1 active site and inhibits its catalytic activity, ultimately leading to Pin1 degradation, which is supported by the requirement of ATRA binding for ATRA-induced Pin1 degradation. These results could help explain why ATRA appeared to be more potent *in vivo* than in enzyme-based assays *in vitro*. Furthermore, the ATRA-Pin1 structures help explain why the new retinoid derivatives fenretinide and bexarotene[33,34] exhibit much lower affinity for Pin1, which may contribute to their failure against solid tumors[35,56,57].

Our findings also provide a strong rationale for developing more potent and specific Pin1-targeted ATRA derivatives for cancer therapy. Comparisons of the Pin1 structures with ATRA and other potent *in vitro* Pin1 inhibitors[27] have identified additional modifications that can be introduced into ATRA to increase its affinity and specificity for Pin1, while reducing its affinity for RARs and possibly improving its half-life. Notably, it is unlikely that ATRA-like Pin1 inhibitors would have major general toxicity due to their selectivity for the active form of Pin1 that is overexpressed in many cancer cells, in addition to the fact that Pin1 KO mice have obvious defects for an extended period of time[25,26]. Indeed, ATRA[37,38] and even liposomal ATRA[60] have not been reported to cause major toxicity.

In summary, we showed that ATRA directly binds, inhibits and ultimately degrades the active form of Pin1 that is overexpressed in many cancer cells to exert potent anticancer activity against APL and TNBC, likely by blocking multiple cancer-driving pathways at once. Since regular ATRA has a short half-life of 45 min with moderate anticancer activity against solid tumors in humans, our results provide a rationale for developing longer half-life ATRA or more potent and specific Pin1-targeted ATRA derivatives for cancer treatment.

Methods are available in Supplemental Materials.

ONLINE METHODS

Cell culture and reagents

293T, HeLa, AU565, BT474, HCC1937, MCF7, MDA-MB-231, MDA-MB-468, SKBR3 and T47D cells (originally obtained from ATCC and maintained in the Lu laboratory) were cultured in Dulbecco's modified Eagle's medium (DMEM), while NB4 cells (obtained from the Pandolfi lab) was cultured in RPMI-1640 and HMLE and MCF10A cells were cultured in F12/DMEM medium. RARα, β, γ triple KO MEFs were from Dr. Hugues de The. All mediums were supplemented with 10% fetal bovine serum (FBS) and all of the cells were cultured at 37°C in a humidified incubator containing 5% CO2. HA-Pin1 was previously described[7,61]. 13cRA, ATRA, EGCG and Juglone were purchased from Sigma. ATRA-releasing pellets were from Innovative Research of America. All mutations were generated by site-directed mutagenesis. Antibodies against various proteins were obtained from the following sources: mouse monoclonal antibodies: Pin1 was previously described[12]; α-tubulin, β-actin, Flag (M2), γ-tubulin (GTU-88) from Sigma; cyclin D1 (DCS-6), SMRT (1212) from Santa Cruz; Smad from BE biosciences (18/Smad2/3); rabbit antibodies: HER2 (C-18), ERα, PML (H-238), RARα (C-20)from Santa Cruz Biotechnology;Akt (9272), c-Jun (9165), PKM2 (3198) from Cell Signaling Technology; NFκB/p65 (EP2161Y) from Epitomics; Cytochrome p450 (2E1) from Abcam; DAPK1 from Sigma. Antibodies against pS71 Pin1 were previously described[7]. AC-93253 and Ro-415253 were purchased from Sigma Aldrich.

Fluorescence polarization-high throughput screen

The N-terminal HiLyte™ Fluor 488-, fluorescein- or TAMRA-labeled peptide had 4 residue sequence core structure of Bth-d-phos.Thr-Pip-Nal, which was synthesized using peptide synthesis companies. This sequence was optimized for solubility and binding to Pin1. A selected set of ~8200 compounds at the Institute for Chemistry and Cell Biology (ICCB-Longwood screening facility) at Harvard Medical School was used as the library source. For the screening assay, a solution containing 250 nM GST-Pin1 or its PPIase, 5 nM labeled peptide, 10 μg/mL bovine serum albumin, 0.01% Tween-20 and 1 mM DTT in a buffer composed of 10 mM HEPES, pH7.4, 10 mM sodium chloride and 1% glycerol at pH 7.4 was used. Measurements of FP and FA were made in black 384-well plates (Corning) using the EnVision reader. Compounds were transferred to plates using a custom-built Seiko pin-transfer robot at the ICCB-Longwood screening facility at Harvard Medical School. The assay can tolerate up to 10% DMSO. The Z' is around 0.70 and consistent for day to day performance. The coefficient of variation is in the range of 4–5%. Candidates were ranked based on Z-score, obtained with the following formula Z score $=(x - \mu)/\sigma$, where: x is the raw score; μ is the mean of the population; σ, is the standard deviation of the population.

Ki values obtained from the FP assay results were derived from Kenakin Ki equation [Kenakin Ki = (Lb)(EC50)(Kd)/(Lo)(Ro)+Lb(Ro-Lo+Lb-Kd)], where Kd [M]: Kd of the probe, EC50 [M]: obtained from FP assay, total tracer Lo [M]: Probe concentration in FP, bound tracer Lb [M]: 85% of probe concentration binds to target protein, total receptor Ro [M]: Pin1 concentration in the FP assay, as described[30].

Photoaffinity Labeling with [^{3}H]ATRA

Photoaffinity labeling of Pin1 with radiolabeled ATRA was performed as described[32], with minor modifications as below. 10 pmol of Pin1 was incubated in microcentrifuge tubes with a series of concentrations of all-trans-[11,12-3H]retinoic acid (PerkinElmer, 43.7 Ci/mmol) in 20 μl of the FP assay buffer at 23°C with agitation for 2 hr in the dark. The caps of the microcentrifuge tubes were opened, and the samples were placed on ice and exposed to Electrophoresis System 365/254 nm UV hand lamp (Fisher Scientific) suspended 6 cm above the surface of the liquid for 15 min. The samples were boiled in SDS sample buffer, followed by separation on standard SDS/PAGE gels. The gels were dried and then used for fluorography at −80°C for 5 days and quantified using Quantity One from BioRad.

PPIase assay

The PPIase activity on GST-Pin1, GST-FKBP12, or GST-cyclophilin in response to 13cRA or ATRA were determined using the chymotrypsin coupled PPIase activity assay with the substrate Suc-Ala-pSer-Pro-Phe-pNA, Suc-Ala-Glu-Pro-Phe-pNA or Suc-Ala-Ala-Pro-Phe-pNA (50 mM) in buffer containing 35 mM HEPES (pH 7.8), 0.2 mM DTT and 0.1 mg/ml BSA, at 10°C, as described previously[5], with the exception that the compounds were preincubated with enzymes for 0.5 to 2 hr at 4°C. Ki value obtained from PPIase assay is derived from Cheng-Prusoff equation [Ki = IC50/ (1 + S/Km)], where Km is the Michaelis constant for the used substrate, S is the initial concentration of the substrate in the assay, and the IC50 value of the inhibitor, as described[62].

Inhibition of cell proliferation

Cells were seeded in a density of 3000 cells per well in 96-well flat-bottomed plates, and incubated for 24 h in 10% FBS-supplemented DMEM culture medium. Cells were then treated with ATRA alone or in combination with other drugs. Control cells received DMSO at a concentration equal to that in drug-treated cells. After 72 h, the number of cells was counted after trypsin digestion, or medium containing 0.5 mg/ml 3-(4,5-dimethylthiazol-2-yl)-2,5-diphenyl-2*H*-tetrazolium bromide was added to each well for 2 h incubation at 37°C, followed by removing the media before adding 200 μl DMSO. Absorbance was determined at 570 nm.

Immunoprecipitation and immunoblotting

Cells were polyethylenimine (PEI)- or lipofemamine-transfected with 8 μg of various plasmids, incubated in 10 cm dishes for 24 h, followed by drug treatment as needed. When harvest, cells were lysed 30 min at 4°C in IP lysis buffer (50 mM HEPES, pH7.4, 150mM NaCl, 1% Tritin X-100, and 10% glycerol) with freshly added phosphatase and protease inhibitors consisting of 100 μM 4-(2-aminoethyl)-benzenesulfonyl fluoride, 80 nM aprotinin, 5 μM bestatin, 1.5 μM E-64 protease inhibitor, 2 μM leupeptin, 1 μM pepstatin A, 2 mM imidazole, 1 mM sodium fluoride, 1 mM sodium molybdate, 1 mM sodium orthovanadate, and 4 mM sodium tartrate dihydrate. After centrifugation at 13,000*g* for 10 min, one tenth of the supernatant was stored as input, and the remainder was incubated 12 h with M2 Flag agarose (Sigma). After brief centrifugation, immunoprecipitates were collected, extensively washed with the aforementioned lysis buffer twice, suspended in 2X

SDS sample buffer (100 mM Tris-HCl, pH 6.8, 4% SDS, 5% β-mercaptoethanol, 20% glycerol, and 0.1% bromphenol blue), boiled for 10 min., and subjected to immunoblotting analysis. Equal amounts of protein were resolved in 15% SDS-polyacrylamide gels. After electrophoresis, gel was transferred to nitrocellulose membranes using a semidry transfer cell. The transblotted membrane was washed twice with Tris-buffered saline containing 0.1% Tween 20 (TBST). After blocking with TBST containing 5% bovine serum albumin (BSA) for 1 h, the membrane was incubated with the appropriate primary antibody (diluted 1:1000) in 2% BSA-containing TBST at 4°C overnight. After incubation with the primary antibody, the membrane was washed three times with TBST for a total of 30 min followed by incubation with horseradish peroxidase (HRP)-conjugated goat anti-rabbit or anti-mouse IgG (diluted 1:2500) for 1 h at room temperature. After three times of extensive wash with TBST for a total of 30 min, the immunoblots were visualized by enhanced chemiluminescence.

Immunostaining and fluorescent microscopy

Human APL samples were kindly provided by Dr. Eduardo Rego from Brazil. Tissue samples were washed with PBS and fixed with 4% paraformaldehyde at room temperature for 20 min, followed by permeabilization and blocking with PBS containing 0.1% Triton X-100 and 5% FBS for 1 h. After another wash with PBS, immunostaining was performed by incubating the cells with mouse anti-Pin1 (Home-made, 1:1000), or rabbit anti-PML (H-238, Santa Cruz; 1:100) primary antibodies at 4°C overnight. Primary antibodies were diluted in PBS containing 0.1% Triton X-100, 0.2% BSA, 0.5 mM PMSF and 1 mM dithiothreitol. After washing with PBS, secondary Alexa Fluor 488-conjugated goat anti-mouse antibodies or Alexa Fluor 564-conjugated goat anti-rabbit antibodies (Invitrogen; 1:200) were added at room temperature for 2 h. Samples were nuclear counterstained with 4,6-diamidino-2-phenylindole (DAPI), mounted and visualized with LSM510 confocal imaging system. For centrosome duplication assays, NIH3T3 cells were used as described previously[7]. Briefly, cells were synchronized in G1/S phase by adding 10 μg/ml aphidicolin for 24 h, then fixed with 4% paraformaldehyde at room temperature for 20 min, and stained for centrosomes with anti-γ-tubulin antibodies (GTU-88, Sigma; 1:100) and analyzed by confocal microscopy.

Immunohistochemistry

Tissue microarrays with a cohort of 48 human TNBC tissues were purchased from US Biomax. Immunohistochemical staining for Pin1 was performed as described previously[23,63]. In brief, deparaffinization and hydration were carried out with xylene, 100%, 75%, 50% ethanol and water sequentially. Antigen retrieval was performed by boiling samples in an autoclave device for 20 min in 1 X antigen retrieval citra (Biogene). Samples were blocked with PBS containing 5% goat serum and 0.1% Triton X-100, followed by incubation with anti-Pin1 antibody (against non-phosphorylated Pin1, 1:200) or anti-DAPK antibody (1:500) at 4 °C in a humidified chamber for 12 h. After extensive washes with PBS, samples were incubated with biotinylated secondary antibody for 2 h and visualized with the Vectastain ABC kit and DAB staining solution (Vector Laboratories). In each sample, expression of Pin1 or DAPK1 was semi-quantified manually in a double-blind manner as high, medium or low according to the standards presented in Figure 6c. The

correlation of Pin1 expression and DAPK1 expression in 48 human TNBC tissues was analyzed by Spearman rank correlation test ($p < 0.001$).

Genome-wide gene expression profiling

Human NB4 cells were treated with 10 μM ATRA (Sigma Aldrich) or doxycycline-induced Pin1 knockdown for 3 days, and total RNA was extracted with the Trizol reagent according to the manufacturer's instructions. Then the samples were processed using Affymetrix GeneChip WT PLUS Reagent Kit, followed by Hybridization Wash and Stain kit. Microarray expression profiles were collected using Affymetrix Human Transcriptome Array 2.0. Original CEL files were analyzed by Affymetrix softwares Expression Console and Transcriptome Analysis Console. Microarray data have been deposited in NCBI Gene Expression Omnibus with series accession number GSE63059. Genes that expressed lower in Pin1 KD or ARTA-treated cells than in VEC or DMSO-treated cells with fold change < 0.5 ($P < 0.05$) were selected as "downregulated" ones, and higher in Pin1 KD or ARTA-treated cells than in VEC or DMSO-treated cells with fold change > 2 ($P < 0.05$) were selected as "upregulated" ones. The array result has been deposited into GEO database (GSE63059) http://www.ncbi.nlm.nih.gov/geo/query/acc.cgi?token=ingnceaardazniz&acc=GSE63059.

Crystallization and complex structure determination for Pin1 PPIase domain with ATRA

Pin1 PPIase domain (residue 51–163) was clone into a pET28a derivative vector with an N-terminal hexahistidine tag followed by recognition sequences by thrombin and PreScission 3C proteases and then followed by the recombinant gene. Mutations of K77Q, K82Q were created by QuikChange™ site directed mutagenesis.

The PPIase K77/82Q was purified similarly to previous published method[29] with minor modification. Briefly, PPIase K77/82Q was overexpressed in *E.coli* BL21 (DE3) strain with isopropyl-β-D-thiogalactopyranoside (IPTG) induction at 16 °C overnight. Cell lysate was first purified with nickel affinity chromatography. The elution was dialysis in buffer of 20 mM HEPES, 100 mM NaCl, 8 mM β-Mercaptoethanol pH 8, while protein is treated with PreScission Protease (GE) over night at 4 °C. After His tag removal, Pin1 PPIase K77/82Q was separated from untruncated protein by a second round of nickel affinity chromatography, and then purified by size exclusion chromatography columns Superdex 75 (GE Healthcare).

Purified PPIase K77/82Q was concentrated to 15 mg/mL. ATRA dissolved in DMSO at the concentration of 1mM was mixed with protein solution and incubated on ice for 3 hours before setting up trays. Incubated protein was co-crystalized by vapor diffusion using a hanging drop of 1 μL protein-ATRA plus 1 μL well solution. The complex formed crystals in 0.2 M ammonium sulfate, 0.1 M HEPES pH7–8.5 and 0.9 M-1.4 M sodium citrate solutions after micro-seeding using apo PPIase domain crystals. The crystals were cryoprotected by addition of 30% glycerol in mother liquor and vitrified in liquid nitrogen before data collection.

X-ray diffraction was collected from synchrotron radiation at beamlines 5.0.2 of the Advanced Light Source (Berkeley, CA) with 3 × 3 CCD array detectors (ADSC Q315R). Data were processed and scaled using the HKL2000 software suite[64]. Data collection statistics are summarized in Supplementary Table 1.

The structure of PPIase K77/82Q bound with ATRA was determined by molecular replacement with PPIase K77/82Q (PDB: 3IKG) as the search model using program Phaser from the CCP4 package suite[65]. The structure was refined with the Refmac5 program from CCP4 package and iterative model building in COOT[66,67]. The final structure was evaluated by both PROCHECK[68] and MolProbity[69]. Refinement statistics are summarized in Supplementary Table 1. The Pin1-ATRA structure was deposited into the Worldwide Protein Data Bank with the PDB code of 4TNS.

Animal studies

For xenograft experiments, 2×10^6 of MDA-MB-231 parent cells or expressing Pin1 or control vectors were injected subcutaneously into flank of 8 weeks-old BALB/c nude mice (Jackson Laboratories). One week later, tumor growth was just about notable by sight, mice were randomly selected to receive ATRA treatment. For intraperitoneal injection, vehicle or 12.5 mg/Kg ATRA were administered three times a week for 8 weeks. For implantation, placebo, 5 or 10 mg 21 day ATRA-releasing pellets (Innovative Research of America) were implanted subcutaneously in the back of nude mice. Tumor sizes were recorded weekly by a caliper for up to 8 weeks and tumor volumes were calculated using formula $L \times W^2 \times 0.52$, where L and W represent length and width, respectively. For NB4 cell transplantation, 8 week-old NOD.Cg-*prkdc*^{scid} *Il2rg*^{tm1Wjl}/SzJ (termed NSG)[70] were used as recipients after sublethal irradiation at 350 Gy. Each mouse was transplanted with 5×10^5 NB4 cells stably expressing Tet-on shPin1 via retro-orbital injection. Five days later when transplanted cells had established, mice were randomly selected to receive regular or doxycycline food and survival curves were recorded. For PML-RARα transgenic cell transplantation, C57BL/6 mice were given 350 Gy irradiation followed by transplantation with 1×10^6 APL cells from hCG-PML-RARα transgenic mice[50,71]. After 5 days when transplanted cells had established, mice were randomly selected to receive placebo (21days placebo-releasing pellets subcutaneously), ATRA (5 mg of 21days ATRA-releasing pellets, subcutaneously), EGCG (12.5mg/kg/day, intraperitoneal), or Juglone (1mg/kg/day, intravenous). Mice were sacrificed after 3 weeks, when APL blast cells appeared in peripheral blood smear of placebo-treated mice. Spleen weight was measured and bone marrow was collected for immunoblotting of PML-RARα and Pin1. Not animals were excluded during the experiments. Animal work was carried out in compliance with the ethical regulations approved by the Animal Care Committee, Beth Israel Deaconess Medical Center, Boston, MA, USA.

Human APL samples

Bone marrow aspirates were obtained with informed consent from the iliac crest of patients in whom the diagnosis of acute promyelocytic leukemia was suspected based on the morphological evaluation of peripheral blood smear. Immediately after the procedure, therapy with ATRA was started[72,73]. Second bone marrow aspirate samples were obtained

on day 3 or 10 of ATRA therapy. Samples tested positive for the PML/RARα rearrangement by RT-PCR. The human sample collection has been approved by the Institutional Review Board at University of São Paulo (HCRP # 13496/2005) or at Tor Vergata University (IRB #12/07).

Statistical analysis

Experiments were routinely repeated at least three times, and the repeat number was increased according to effect size or sample variation. We estimated the sample size considering the variation and mean of the samples. No statistical method was used to predetermine sample size. No animals or samples were excluded from any analysis. Animals were randomly assigned groups for *in vivo* studies; no formal randomization method was applied when assigning animals for treatment. Group allocation and outcome assessment was not done in a blinded manner, including for animal studies. All data are presented as the means ± SD, followed by determining significant differences using the two-tailed student *t* test or ANOVA test, where *P < 0.05, **P < 0.01, ***P < 0.001.

Supplementary Material

Refer to Web version on PubMed Central for supplementary material.

Acknowledgments

We thank anonymous reviewers for improving manuscript, W. G. Kaelin Jr. J. Clardy, N. Gray and A. Chakraborty for constructive advice, P. A. Chambon (Université de Strasbourg) and H. de The (Institut National de la Santé et de la Recherche Médicale) for RARα, β, γ triple KO MEFs, C. Ng for assistance with immunostaining and T. Garvey for editing the manuscript. S. W. is a recipient of Susan G. Komen for the Cure postdoctoral fellow (KG111233). The work is supported by grants from US National Institutes of Health R01CA167677, R03DA031663 and R01HL111430 (K. P. L.).

References

1. Hanahan D, Weinberg RA. Hallmarks of cancer: the next generation. Cell. 2011; 144:646–674. [PubMed: 21376230]
2. Lu KP, Zhou XZ. The prolyl isomerase Pin1: a pivotal new twist in phosphorylation signalling and human disease. Nat Rev Mol Cell Biol. 2007; 8:904–916. [PubMed: 17878917]
3. Lu Z, Hunter T. Pin1 and cancer. Cell Res. 2014; 24:1033–1049. [PubMed: 25124924]
4. Lu KP, Finn G, Lee TH, Nicholson LK. Prolyl cis-trans isomerization as a molecular timer. Nature Chem Biol. 2007; 3:619–629. [PubMed: 17876319]
5. Yaffe MB, et al. Sequence-specific and phosphorylation-dependent proline isomerization: A potential mitotic regulatory mechanism. Science. 1997; 278:1957–1960. [PubMed: 9395400]
6. Nakamura K, et al. Proline isomer-specific antibodies reveal the early pathogenic tau conformation in Alzheimer's disease. Cell. 2012; 149:232–244. [PubMed: 22464332]
7. Lee TH, et al. Death associated protein kinase 1 phosphorylates Pin1 and inhibits its prolyl isomerase activity and cellular function. Mol Cell. 2011; 22:147–159. [PubMed: 21497122]
8. Li Q, et al. The rs2233678 Polymorphism in PIN1 Promoter Region Reduced Cancer Risk: A Meta-Analysis. PLoS One. 2013; 8:e68148. [PubMed: 23874525]
9. Wulf G, Garg P, Liou YC, Iglehart D, Lu KP. Modeling breast cancer in vivo and ex vivo reveals an essential role of Pin1 in tumorigenesis. EMBO J. 2004; 23:3397–3407. [PubMed: 15257284]
10. Suizu F, Ryo A, Wulf G, Lim J, Lu KP. Pin1 regulates centrosome duplication and its overexpression induces centrosome amplification, chromosome instability and oncogenesis. Mol Cell Biol. 2006; 26:1463–1479. [PubMed: 16449657]

11. Wulf GM, et al. Pin1 is overexpressed in breast cancer and potentiates the transcriptional activity of phosphorylated c-Jun towards the cyclin D1 gene. EMBO J. 2001; 20:3459–3472. [PubMed: 11432833]
12. Liou YC, et al. Loss of Pin1 function in the mouse causes phenotypes resembling cyclin D1-null phenotypes. Proc Natl Acad Sci USA. 2002; 99:1335–1340. [PubMed: 11805292]
13. Ryo A, et al. Regulation of NF-kappaB signaling by Pin1-dependent prolyl isomerization and ubiquitin-mediated proteolysis of p65/RelA. Mol Cell. 2003; 12:1413–1426. [PubMed: 14690596]
14. Lam PB, et al. Prolyl isomerase Pin1 is highly expressed in Her2-positive breast cancer and regulates erbB2 protein stability. Mol Cancer. 2008; 7:91. [PubMed: 19077306]
15. Stanya KJ, Liu Y, Means AR, Kao HY. Cdk2 and Pin1 negatively regulate the transcriptional corepressor SMRT. J Cell Biol. 2008; 183:49–61. [PubMed: 18838553]
16. Liao Y, et al. Peptidyl-prolyl cis/trans isomerase Pin1 is critical for the regulation of PKB/Akt stability and activation phosphorylation. Oncogene. 2009; 28:2436–2445. [PubMed: 19448664]
17. Nakano A, et al. Pin1 downregulates TGF-beta signaling by inducing degradation of Smad proteins. J Biol Chem. 2009; 284:6109–6115. [PubMed: 19122240]
18. Rajbhandari P, et al. Regulation of estrogen receptor alpha N-terminus conformation and function by peptidyl prolyl isomerase Pin1. Mol Cell Biol. 2012; 32:445–457. [PubMed: 22064478]
19. Yang W, et al. ERK1/2-dependent phosphorylation and nuclear translocation of PKM2 promotes the Warburg effect. Nat Cell Biol. 2012; 14:1295–1304. [PubMed: 23178880]
20. Min SH, et al. Negative regulation of the stability and tumor suppressor function of fbw7 by the pin1 prolyl isomerase. Mol Cell. 2012; 46:771–783. [PubMed: 22608923]
21. Luo ML, et al. Prolyl isomerase Pin1 acts downstream of miR200c to promote cancer stem-like cell traits in breast cancer. Cancer Res. 2014; 74:3603–3616. [PubMed: 24786790]
22. Luo ML, et al. The Rab2A GTPase is a breast cancer stem-promoting gene that enhances tumorigenesis via activating Erk signaling. Cell Rep. 2015 in press.
23. Rustighi A, et al. Prolyl-isomerase Pin1 controls normal and cancer stem cells of the breast. EMBO molecular medicine. 2014; 6:99–119. [PubMed: 24357640]
24. Lu KP. Prolyl isomerase Pin1 as a molecular target for cancer diagnostics and therapeutics. Cancer Cell. 2003; 4:175–180. [PubMed: 14522251]
25. Fujimori F, Takahashi K, Uchida C, Uchida T. Mice lacking Pin1 develop normally, but are defective in entering cell cycle from G(0) arrest. Biochem Biophys Res Commun. 1999; 265:658–663. [PubMed: 10600477]
26. Liou YC, et al. Role of the prolyl isomerase Pin1 in protecting against age-dependent neurodegeneration. Nature. 2003; 424:556–561. [PubMed: 12891359]
27. Moore JD, Potter A. Pin1 inhibitors: Pitfalls, progress and cellular pharmacology. Bioorg Med Chem Lett. 2013; 23:4283–4291. [PubMed: 23796453]
28. Bialik S, Kimchi A. The death-associated protein kinases: structure, function, and beyond. Annu Rev Biochem. 2006; 75:189–210. [PubMed: 16756490]
29. Zhang Y, et al. Structural basis for high-affinity peptide inhibition of human Pin1. ACS Chem Biol. 2007; 2:320–328. [PubMed: 17518432]
30. Auld, DS., et al. Receptor Binding Assays for HTS and Drug Discovery. In: Sittampalam, GS., et al., editors. Assay Guidance Manual. Bethesda (MD): 2004.
31. Chen H, Juchau MR. Recombinant human glutathione S-transferases catalyse enzymic isomerization of 13-cis-retinoic acid to all-trans-retinoic acid in vitro. Biochem J. 1998; 336 (Pt 1): 223–226. [PubMed: 9806904]
32. Bernstein PS, Choi SY, Ho YC, Rando RR. Photoaffinity labeling of retinoic acid-binding proteins. Proc Natl Acad Sci U S A. 1995; 92:654–658. [PubMed: 7846032]
33. Moon RC, et al. N-(4-Hydroxyphenyl)retinamide, a new retinoid for prevention of breast cancer in the rat. Cancer Res. 1979; 39:1339–1346. [PubMed: 421218]
34. Boehm MF, et al. Design and synthesis of potent retinoid X receptor selective ligands that induce apoptosis in leukemia cells. J Med Chem. 1995; 38:3146–3155. [PubMed: 7636877]

35. Connolly RM, Nguyen NK, Sukumar S. Molecular pathways: current role and future directions of the retinoic acid pathway in cancer prevention and treatment. Clin Cancer Res. 2013; 19:1651–1659. [PubMed: 23322901]
36. Huang ME, et al. Use of all-trans retinoic acid in the treatment of acute promyelocytic leukemia. Blood. 1988; 72:567–572. [PubMed: 3165295]
37. de The H, Chen Z. Acute promyelocytic leukaemia: novel insights into the mechanisms of cure. Nat Rev Cancer. 2010; 10:775–783. [PubMed: 20966922]
38. Sanz MA, Lo-Coco F. Modern approaches to treating acute promyelocytic leukemia. J Clin Oncol. 2011; 29:495–503. [PubMed: 21220600]
39. Nasr R, et al. Eradication of acute promyelocytic leukemia-initiating cells through PML-RARA degradation. Nat Med. 2008; 14:1333–1342. [PubMed: 19029980]
40. Ablain J, et al. Uncoupling RARA transcriptional activation and degradation clarifies the bases for APL response to therapies. J Exp Med. 2013; 210:647–653. [PubMed: 23509325]
41. Langenfeld J, Kiyokawa H, Sekula D, Boyle J, Dmitrovsky E. Posttranslational regulation of cyclin D1 by retinoic acid: a chemoprevention mechanism. Proc Natl Acad Sci U S A. 1997; 94:12070–12074. [PubMed: 9342364]
42. Tsai YC, et al. Effects of all-trans retinoic acid on Th1- and Th2-related chemokines production in monocytes. Inflammation. 2008; 31:428–433. [PubMed: 18989765]
43. Sheng N, et al. Retinoic acid regulates bone morphogenic protein signal duration by promoting the degradation of phosphorylated Smad1. Proc Natl Acad Sci U S A. 2010; 107:18886–18891. [PubMed: 20956305]
44. Lanotte M, et al. NB4, a maturation inducible cell line with t(15;17) marker isolated from a human acute promyelocytic leukemia (M3). Blood. 1991; 77:1080–1086. [PubMed: 1995093]
45. Brondani V, Schefer Q, Hamy F, Klimkait T. The peptidyl-prolyl isomerase Pin1 regulates phospho-Ser77 retinoic acid receptor alpha stability. Biochem Biophys Res Commun. 2005; 328:6–13. [PubMed: 15670742]
46. Gausdal G, et al. Cyclic AMP can promote APL progression and protect myeloid leukemia cells against anthracycline-induced apoptosis. Cell Death Dis. 2013; 4:e516. [PubMed: 23449452]
47. Uchida T, et al. Pin1 and Par14 peptidyl prolyl isomerase inhibitors block cell proliferation. Chemistry & biology. 2003; 10:15–24. [PubMed: 12573694]
48. Urusova DV, et al. Epigallocatechin-gallate suppresses tumorigenesis by directly targeting Pin1. Cancer Prev Res (Phila). 2011; 4:1366–1377. [PubMed: 21750208]
49. Hennig L, et al. Selective inactivation of parvulin-like peptidyl-prolyl cis/trans isomerases by juglone. Biochemistry. 1998; 37:5953–5960. [PubMed: 9558330]
50. He LZ, et al. Acute leukemia with promyelocytic features in PML/RARalpha transgenic mice. Proc Natl Acad Sci U S A. 1997; 94:5302–5307. [PubMed: 9144232]
51. Song MS, et al. The deubiquitinylation and localization of PTEN are regulated by a HAUSP-PML network. Nature. 2008; 455:813–817. [PubMed: 18716620]
52. Budd GT, et al. Phase I/II trial of all-trans retinoic acid and tamoxifen in patients with advanced breast cancer. Clin Cancer Res. 1998; 4:635–642. [PubMed: 9533531]
53. Muindi J, et al. Continuous treatment with all-trans retinoic acid causes a progressive reduction in plasma drug concentrations: implications for relapse and retinoid “resistance” in patients with acute promyelocytic leukemia. Blood. 1992; 79:299–303. [PubMed: 1309668]
54. Kogan SC, Hong SH, Shultz DB, Privalsky ML, Bishop JM. Leukemia initiated by PMLRARalpha: the PML domain plays a critical role while retinoic acid-mediated transactivation is dispensable. Blood. 2000; 95:1541–1550. [PubMed: 10688806]
55. Arrieta O, et al. Randomized phase II trial of All-trans-retinoic acid with chemotherapy based on paclitaxel and cisplatin as first-line treatment in patients with advanced non-small-cell lung cancer. J Clin Oncol. 2010; 28:3463–3471. [PubMed: 20547984]
56. Ramlau R, et al. Randomized phase III trial comparing bexarotene (L1069-49)/cisplatin/vinorelbine with cisplatin/vinorelbine in chemotherapy-naive patients with advanced or metastatic non-small-cell lung cancer: SPIRIT I. J Clin Oncol. 2008; 26:1886–1892. [PubMed: 18398154]

57. Decensi A, et al. Randomized double-blind 2 × 2 trial of low-dose tamoxifen and fenretinide for breast cancer prevention in high-risk premenopausal women. J Clin Oncol. 2009; 27:3749–3756. [PubMed: 19597031]
58. Muindi JR, et al. Clinical pharmacology of oral all-trans retinoic acid in patients with acute promyelocytic leukemia. Cancer Res. 1992; 52:2138–2142. [PubMed: 1559217]
59. Gianni M, et al. Inhibition of the peptidyl-prolyl-isomerase Pin1 enhances the responses of acute myeloid leukemia cells to retinoic acid via stabilization of RAR{alpha} and PML-RAR{alpha}. Cancer Res. 2009; 69:1016–1026. [PubMed: 19155306]
60. Jain P, et al. Single-agent liposomal all-trans-retinoic Acid as initial therapy for acute promyelocytic leukemia: 13-year follow-up data. Clinical lymphoma, myeloma & leukemia. 2014; 14:e47–49.
61. Lu PJ, Zhou XZ, Liou YC, Noel JP, Lu KP. Critical role of WW domain phosphorylation in regulating its phosphoserine-binding activity and the Pin1 function. J Biol Chem. 2002; 277:2381–2384. [PubMed: 11723108]
62. Wildemann D, et al. Nanomolar Inhibitors of the Peptidyl Prolyl Cis/Trans Isomerase Pin1 from Combinatorial Peptide Libraries. J Med Chem. 2006; 49:2147–2150. [PubMed: 16570909]
63. Ryo A, Nakamura N, Wulf G, Liou YC, Lu KP. Pin1 regulates turnover and subcellular localization of beta-catenin by inhibiting its interaction with APC. Nature Cell Biol. 2001; 3:793–801. [PubMed: 11533658]
64. Otwinowski Z, Minor W. Methods Enzymol. 1997; 276:472–494.
65. Bailey SM. The CCP4 suite: programs for protein crystallography. Acta Crystallogr D Biol Crystallogr. 1994; 50:760–763. [PubMed: 15299374]
66. Emsley P, Cowtan K. Coot: model-building tools for molecular graphics. Acta Crystallogr D Biol Crystallogr. 2004; 60:2126–2132. [PubMed: 15572765]
67. Emsley P, Lohkamp B, Scott WG, Cowtan K. Features and development of Coot. Acta Crystallogr D Biol Crystallogr. 2010; 66:486–501. [PubMed: 20383002]
68. Laskowski RA, Moss DS, Thornton JM. Main-chain bond lengths and bond angles in protein structures. J Mol Biol. 1993; 231:1049–1067. [PubMed: 8515464]
69. Chen VB, et al. MolProbity: all-atom structure validation for macromolecular crystallography. Acta Crystallogr D Biol Crystallogr. 2010; 66:12–21. [PubMed: 20057044]
70. Shultz LD, et al. Human lymphoid and myeloid cell development in NOD/LtSz-scid IL2R gamma null mice engrafted with mobilized human hemopoietic stem cells. J Immunol. 2005; 174:6477–6489. [PubMed: 15879151]
71. dos Santos GA, et al. (+)alpha-Tocopheryl succinate inhibits the mitochondrial respiratory chain complex I and is as effective as arsenic trioxide or ATRA against acute promyelocytic leukemia in vivo. Leukemia. 2012; 26:451–460. [PubMed: 21869839]
72. Lo-Coco F, et al. Retinoic acid and arsenic trioxide for acute promyelocytic leukemia. N Engl J Med. 2013; 369:111–121. [PubMed: 23841729]
73. Rego EM, et al. Improving acute promyelocytic leukemia (APL) outcome in developing countries through networking, results of the International Consortium on APL. Blood. 2013; 121:1935–1943. [PubMed: 23319575]

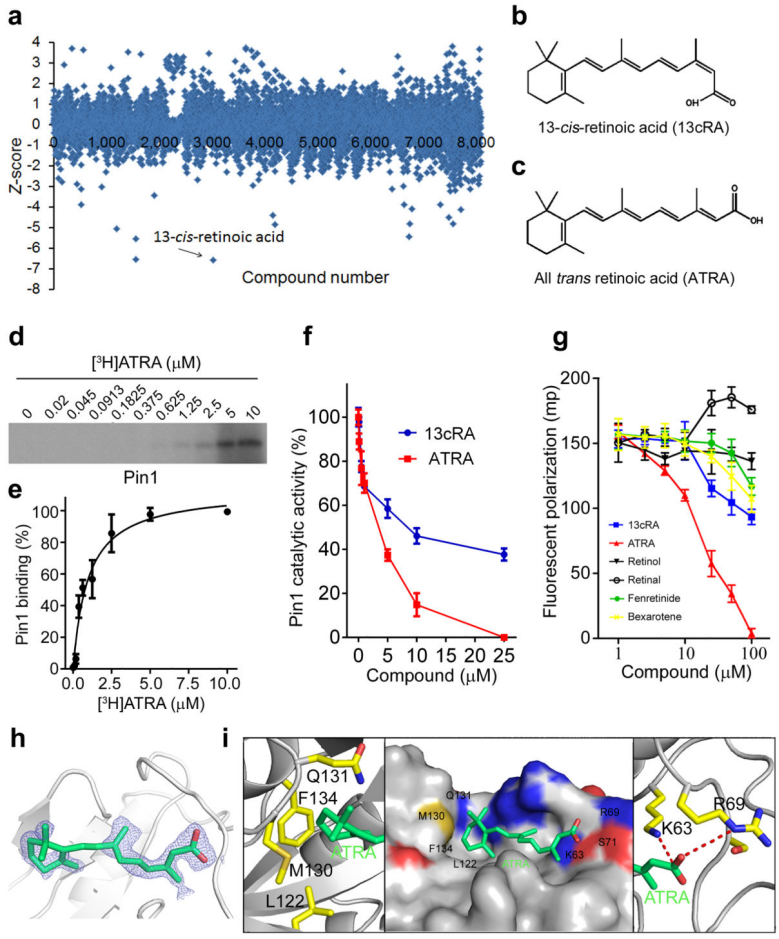

Figure 1. Mechanism-based screening identifies ATRA as a submicromolar Pin1 inhibitor binding to the Pin1 active site

(**a**) Summary plot of FP-HTS for Pin1 inhibitors, with 13-*cis*-retinoic acid having lowest Z score, as determined by folds of standard deviation below the mean of each screening plate.

(**b** and **c**) Structures of *cis* (13cRA) (**b**) and *trans* (ATRA) (**c**) of retinoic acid.

(d and **e)** [^{3}H]ATRA binding to Pin1 in a dose-dependent manner. Pin1 was incubated with various concentrations of [^{3}H]ATRA, followed by UV exposure before SDS-gel and radiography (**d**). Pin1-bound [^{3}H]ATRA signals were quantified and plotted against ATRA concentrations (**e**) (mean ± s.d. of three experiments).

(**f**) Inhibition of Pin1 catalytic activity by ATRA or 13cRA, as measured by PPIase assay (mean ± s.d. of two experiments).

(**g**) pTide- HiLyte^{TM} Fluor 488 was added to Pin1, followed by incubation of different concentrations of compounds indicated for 0.5 hour, before FP readout (mean ± s.d. of three experiments).

(**h** and **i**) After ATRA soaking, strong electron density was observed at the Pin1 active site in the co-crystal (**h**). X-ray diffraction of the ATRA-Pin1 co-crystal structure was collected from synchrotron radiation and data were processed and scaled using the HKL2000 software suite (**i**). ATRA-Pin1 binding (middle) is mediated by salt bridges between the carboxylic acid of ATRA and K63 and R69 residues (right), as well as by hydrophobic interaction

between aromatic moiety of ATRA and L122, M130, Q131 and F134 residues (left). The PDB code for the Pin1-ATRA structure is 4TNS.

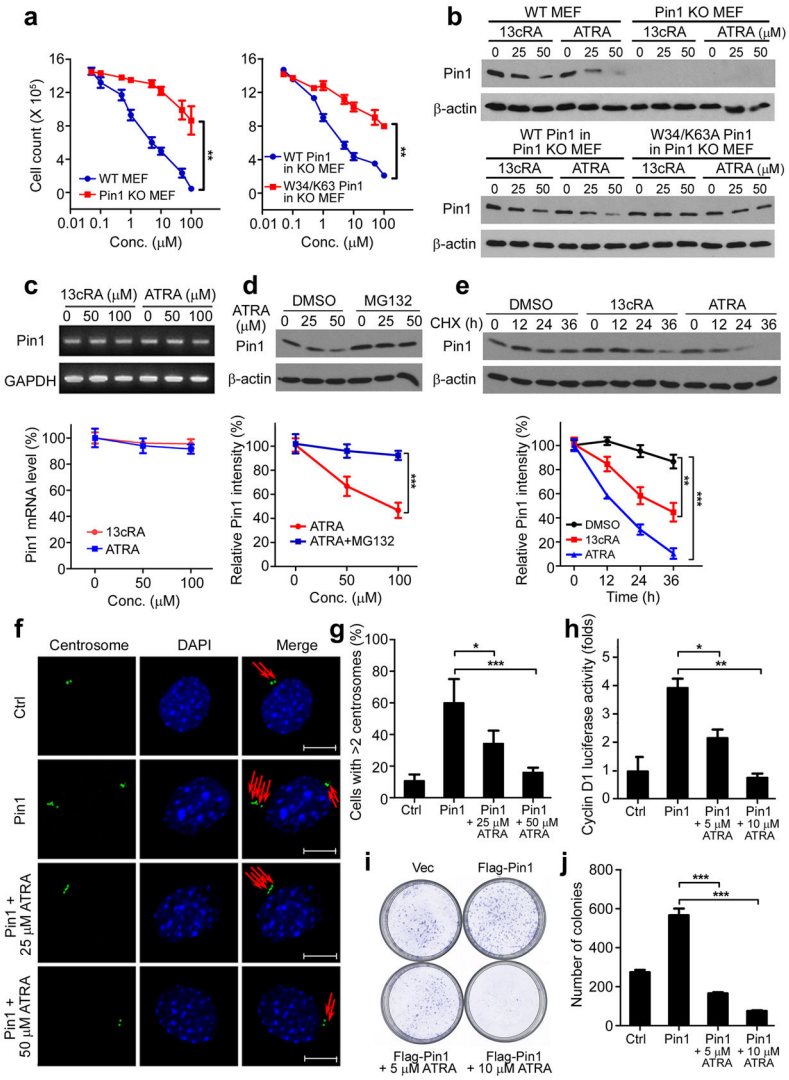

Figure 2. ATRA causes Pin1 degradation and inhibits its oncogenic function in cells

(**a**) WT and Pin1 KO MEFs (left) or Pin1 KO MEFs reconstituted with WT- or W34/K63A-Pin1 (right) were treated with indicated concentrations of ATRA for 72 h, followed by MTT cell growth assay with the readout absorbance measured by 570 nm (mean ± s.d. of three experiments)

(**b**) WT and Pin1 KO MEFs (upper) or Pin1 KO MEFs reconstituted with WT- or W34/K63A-Pin1 (lower) were treated with the indicated concentrations of13cRA or ATRA for 72 h. Pin1 abundance was assessed by immunoblotting (mean ± s.d. of three experiments).

(**c**) MEFs were treated with the indicated concentrations of ATRA or 13cRA for 72h, followed by quantitative RT-PCR to detect Pin1 mRNA. Top panel shows representative gel, and bottom graph shows quantification (mean ± s.d. of three experiments).

(**d**) MEFs were treated with the indicated concentrations of ATRA for 48 h followed by co-treatment of 10 μM MG132 or DMSO control for additional 24 h before harvest. Pin1 abundance was measured by immunoblotting. Top panel shows representative gel, and bottom graph shows quantification (mean ± s.d. of three experiments).

(**e**) MEFs were treated with 50 μM ATRA, 50 μM 13cRA or DMSO control for 24h, followed by cycloheximide (CHX) chase for the indicated times. Pin1 abundance was measured by immunoblotting. Top panel shows representative gel, and bottom graph shows quantification (mean ± s.d. of three experiments).

(**f** and **g**) NIH3T3 cells stably expressing Flag-tagged Pin1 or empty vector (Ctrl) were treated with indicated concentrations of ATRA for 72 h, followed by immunostaining with antibodies specific for γ-tubulin to detect centrosomes (red arrow). Scale bar, 10μM. Cells containing over 2 centrosomes were quantified from 3 independent experiments with over 100 cells in each (**g**).

(**h**) SKBR3 cells were co-transfected with a cyclin D1 promoter-driven luciferase construct, and with Flag-Pin1 or control vector. Cells were treated with indicated concentrations of ATRA for 72 h. Luciferase activity was measured by reporter gene assay (mean ± s.d. of three experiments).

(**i** and **j**) SKBR3 cells were co-transfected with Flag-Pin1 or empty vector, and were then treated with indicated concentrations of ATRAfor 48 h. Foci formation assay was applied. Representative image (**i**), foci quantification in (**j**) (mean ± s.d. of three experiments).

*P < 0.05, **P < 0.01, ***P < 0.001, as determined by Student's t-test.

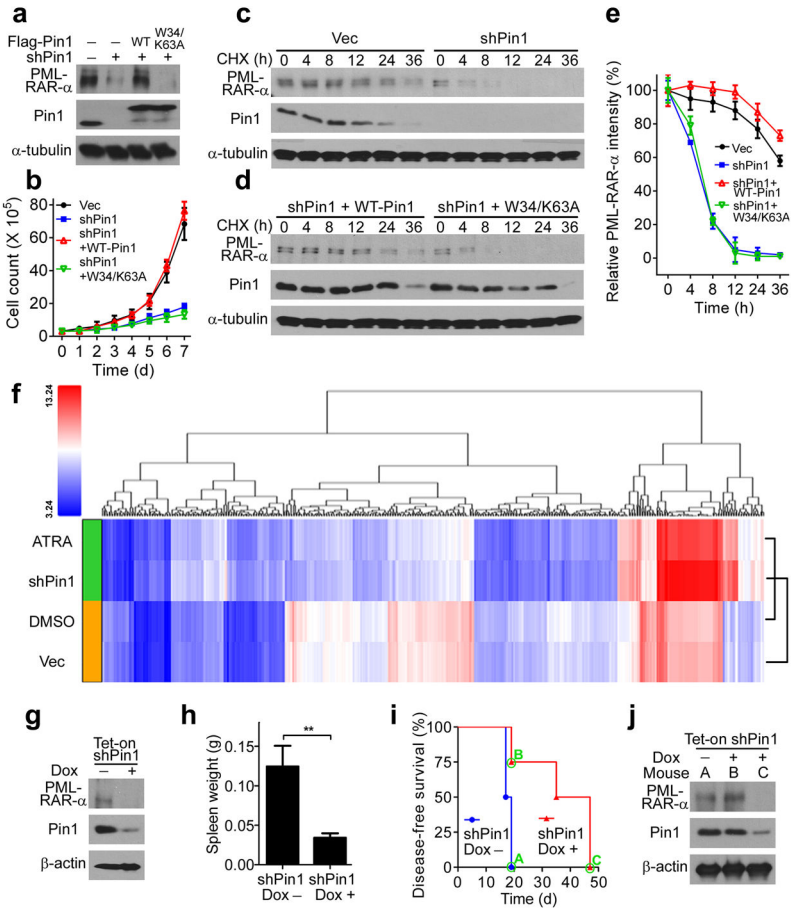

Figure 3. Pin1 is a critical target for ATRA to induce PML-RARα degradation and inhibit proliferation in APL cells

(**a** and **b**) NB4 cells were stably infected by lentivirus expressing shPin1 and WT or W34/K63A Flag-Pin1, followed by IB for PML-RARα or Pin1 (**a**) or counting cell number over time (**b**) (mean ± s.d. of three experiments).

(**c–e**) NB4 cells stably infected by lentivirus expressing shPin1 and WT or W34/K63A Flag-Pin1were subjected to the CHX chase, followed by IB for PML-RARα and Pin1 (**c** and **d**), with quantification in (**e**) (mean ± s.d. of three experiments).

(**f**) Hierarchical cluster of the differential expression profiling showed similar profiles in ATRA-treated and Pin1 KDNB4 cells. NB4 cells were ATRA- or DMSO-treated for 72 h, or doxycycline (shPin1)- or mock (vec)-induced shPin1 KD for 72 h, followed by extracting mRNAs and microarray analysis. Fold changes are color-coded shown in the bar.

(**g–j**) Immunodeficient NSG mice were transplanted with 5×10^5 human APL NB4 cells stably carrying inducible Tet-on shPin1 and, 5 days after, received doxycycline food to induce Pin1 KD, followed by examining PML-RARα and Pin1 in the bone marrow (**g**), spleen size (**h**) (mean ± s.d. of four mice) and disease-free survival (**i**) of transplanted mice. Bone marrow samples from the mice labeled with A, B, C in panel **o** were subjected to IB for PML-RARα and Pin1 (**j**).

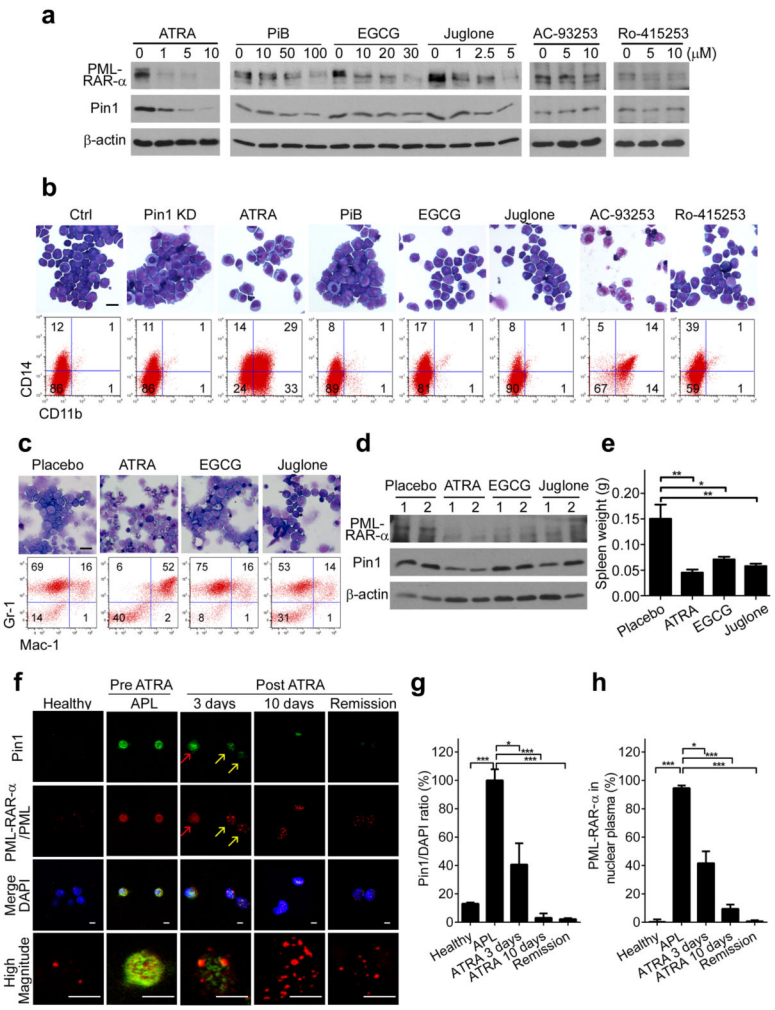

Figure 4. Inhibition of Pin1 by ATRA or other compounds causes PML-RARα degradation and treats APL in cell and mouse models and even human patients

(**a** and **b**) NB4 cells were treated with ATRA, various Pin1 inhibitors, RAR inhibitor or RAR activator for 72 h, followed by IB for PML-RARα and Pin1 (**b**), or Giemsa staining (**b**, upper panels) or FACS with CD14 and CD11b (**b**, lower panels) for detecting APL cell differentiation. Scale bar, 10μM.

(**c–e**) Sublethally irradiated C57BL/6J mice were transplanted with 1×10^6 APL cells isolated from hCG-PML-RARα transgenic mice and, 5 days later, treated with ATRA-releasing implants, EGCG, Juglone or placebo for 3 weeks, followed by determining APL cell differentiation status with Giemsa staining (upper) or FACS with Gr-1 and Mac-1 (lower) (**c**), PML-RARα and Pin1 expression in the bone marrow (**d**), and the size of the spleen in mice (**e**) (mean ± s.d. of ten mice). Mac-1 is the same to CD11b. Scale bar, 10μM.

(**f–h**) Bone marrow samples from healthy controls (n=24) or APL patients before (n=19) or after the treatment with ATRA for 3 (n=3) or 10 days (n=3) or APL patients in complete remission (n=17) were immunostained with anti-Pin1 and anti-PML antibodies (**f**). Relative levels of Pin1 (**g**) in the nucleus and PML-RARα in the nuclear plasma outside of the PML nuclear body (**h**) were semi-quantified (mean ± s.d.). Red arrows, PML-RARα/PML

diffusely distributed to the entire nucleus in APL cells containing more Pin1; yellow arrows, PML-RARα/PML localized to the PML body in APL cells containing less Pin1. Scale bar, 5μM.

*P < 0.05, **P < 0.01, ***P < 0.001, as determined by Student's t-test.

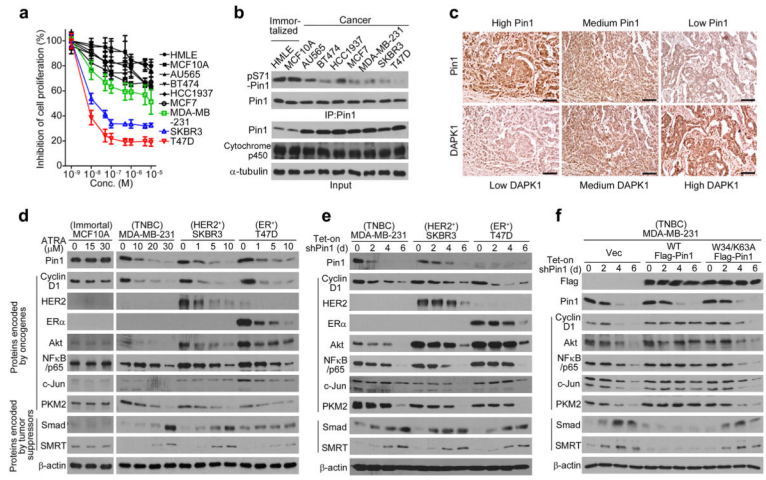

Figure 5. ATRA ablates the active Pin1 and thereby turns off oncogenes and turns on tumor suppressors in breast cancer

(**a** and **b**) Human normal and breast cancer cells were either treated with ATRA for 72 h, followed by assaying colorimetric MTT assay (**a**) (mean ± s.d. of three experiments) or directly subjected without the treatment to IP/IB for detecting Pin1 and its S71 phosphorylation (**b**).

(**c**) An inverse correlation of Pin1 and DAPK1 in human TNBC tissues (**d**), with quantification in (**e**) (n=48). Scale bar, 50μM.

(**d–f**) Different breast cells were treated with different concentration of ATRA for 72 hr (**d**) or different breast cells stably expressing Tet-inducible Pin1 shRNA were treated with tetracycline for different times to induce Pin1 KD (**e**), or after reconstitution of shRNA-resistant Pin1 or its W34/K63A mutant (**f**), followed by IB for detecting different proteins.

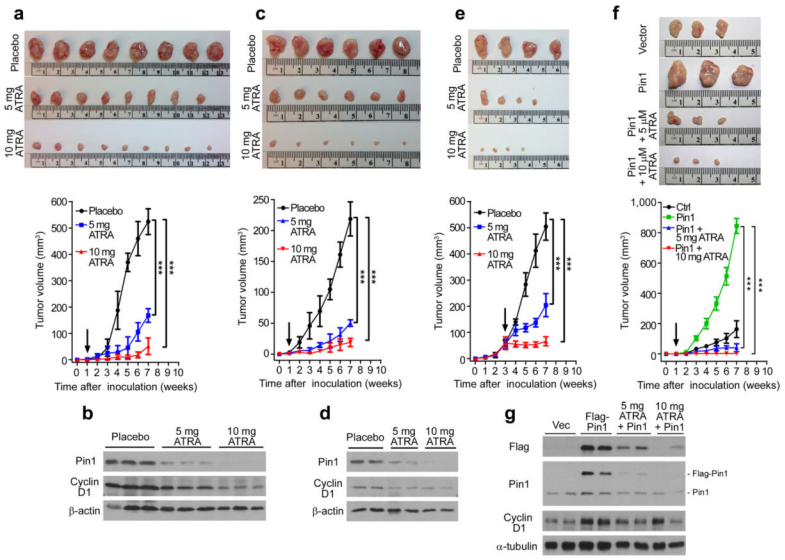

Figure 6. ATRA exerts potent anticancer activity against TNBC *in vivo* by ablating Pin1 and thereby blocking multiple cancer pathways simultaneously

(**a–d**) Nude mice were flank-inoculated with 2 × 10^6 MDA-MB-231 cells (**a** and **b**) or MDA-MB-468 cells (**c** and **d**), 1 week later, implanted with 5 or 10 mg 21 day ATRA-releasing or placebo pellets. Tumor sizes were weekly measured and mice were sacrificed after 7 weeks to collect tumor tissues (**a**, **c**, upper). Curves of tumor volume were plotted over time (**a**, **c**, lower) (mean ± s.d. of eight mice for **a**, six mice for **c**). Pin1 and cyclin D1 in xenograft tumors were assayed by IB (**b** and **d**).

(**e**) Nude mice were flank-inoculated with 2 × 10^6 MDA-MB-231 cells and, 3 week later (arrow), implanted with 5 or 10 mg 21 day ATRA-releasing or placebo pellets. Tumor sizes were weekly measured and mice were sacrificed after 4 weeks to collect tumor tissues (**upper**). Curves of tumor volume were plotted over time (**lower**) (mean ± s.d. of four mice).

(**f** and **g**) MDA-MB-231 cells stably expressing Flag-Pin1 or control vector were inoculated into nude mice, and 1 week later treated with ATRA implants for 7 weeks before collecting tumors (**f**, upper) Quantitative curves of tumor volume were plotted (**f**, lower) (mean ± s.d. of three mice). Exogenous and endogenous Pin1 along cyclin D1 in xenograft tumors were assayed by IB (**g**).

*P < 0.05, **P < 0.01, ***P < 0.001, as determined by Student's t-test.